JGR Atmospheres

RESEARCH ARTICLE
10.1029/2019JD030751

Spatiotemporal Variation in Presummer Precipitation Over South China From 1979 to 2015 and Its Relationship With Urbanization

Lin Su[1], Junlu Li[1], Xiaoming Shi[1], and Jimmy C. H. Fung[1,2]

[1]Division of Environment and Sustainability, The Hong Kong University of Science and Technology, Hong Kong, [2]Department of Mathematics, The Hong Kong University of Science and Technology, Hong Kong

Key Points:

- The presummer precipitation over South China had undergone a drastic intensification between 1979 and 2015
- The increasing trend was much more significant in urban areas than in nonurban areas
- The effects of urbanization on the intensification of the presummer precipitation over South China were analyzed and discussed

Correspondence to:
J. C. H. Fung,
majfung@ust.hk

Citation:
Su, L., Li, J., Shi, X., & Fung, J. C. H. (2019). Spatiotemporal variation in presummer precipitation over South China from 1979 to 2015 and its relationship with urbanization. *Journal of Geophysical Research: Atmospheres*, *124*, 6737–6749. https://doi.org/10.1029/2019JD030751

Received 5 APR 2019
Accepted 9 JUN 2019
Accepted article online 18 JUN 2019
Published online 3 JUL 2019

Abstract The variation in presummer precipitation in South China from 1979 to 2015 and its relationship with urbanization were analyzed. The results reveal that the intensity of precipitation and the occurrence of extreme precipitation events during the presummer season in South China have increased significantly, and the upward trend is much more significant in urban areas than in nonurban areas. The mean trends in urban and nonurban areas in South China are, respectively, 1.34 and 0.97 mm/day/year for maximum daily precipitation, 4.41 and 2.79 mm/year for the top 5% of daily precipitation, and 0.26 and 0.16 day/year for extremely heavy precipitation days during the presummer season. In addition to the variability of large-scale atmospheric circulation, urbanization appears to have a significant effect on the variability of presummer precipitation in South China, especially with regard to the intensity of precipitation and the occurrence of extremely heavy precipitation. From 1979 to 2015, the upward trends of maximum daily precipitation, the top 5% of daily precipitation, and extremely heavy precipitation days during presummer season in urban areas are, respectively, between 38.14% and 39.18%, 55.97% and 59.14%, and 43.75% and 68.75% higher than those in nonurban areas during the investigated period. Urban areas in South China are more exposed to extreme precipitation than nonurban areas during the presummer season.

1. Introduction

Based on satellite observations and numerical simulations, extreme precipitation events have become more and more frequent against the background of global warming (Allan & Soden, 2008; Kunkel et al., 1999; Madsen et al., 2014; Zhai et al., 2005; Wang & Zhou, 2005). Moreover, precipitation has been reported to be significantly altered by feedback from local land surface processes in specific types of land cover, such as urban areas (Huff & Changnon, 1973; Li et al., 2015; Shastri et al., 2015; Wang et al., 2015; Wai et al., 2017; Liang & Ding, 2017; Niyogi et al., 2017). Urban heat islands can induce updrafts, which dynamically trigger moist convection, resulting in precipitation in downwind regions under favorable thermodynamic conditions (Baik, 1992; Han & Baik, 2008). Higher surface roughness can also lead to changes in airflow, inhibiting or enhancing precipitating convective systems when passing through urban areas (Bornstein & LeRoy, 1990; Tumanov et al., 1999).

South China (109–118°E, 20–26°N; Figure 1), including Guangdong province (GD) and parts of Guangxi, Hunan, Jiangxi, and Fujian provinces, has experienced drastically rapid urbanization in the last 40 years, as shown in Figure 2. The Pearl River Delta (PRD) region (highlighted by the thickened boundary in Figure 1), located in the middle of South China, is one of the most urbanized areas in China (Tse et al., 2018).

South China has the highest annual precipitation in the entire nation, with a rainy season from April to September. Precipitation in South China is affected by complex terrain, land-sea contrast, monsoons, and typhoons (Yu et al., 2007). Dominated by a typical subtropical marine monsoon climate, precipitation in South China is directly affected by the activity of the East Asian monsoon. Large amounts of water vapor are transported from the ocean to South China during the establishment of the East Asian summer monsoon and encounter with frontal systems in South China during the presummer season (April to June), resulting in frequent severe convective precipitation events (Chen et al., 2011) and contributing to the first flood period in the presummer season in South China (Huang, 1986). Precipitation during the presummer season

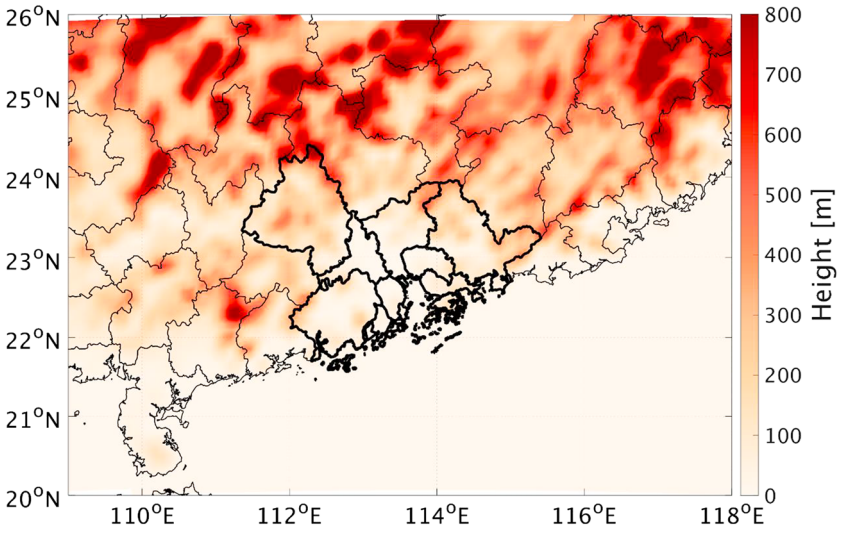

Figure 1. Terrain height of South China.

accounts for about 50% or more of the total annual precipitation in South China (Qiang & Yang, 2008). Compared with typhoon precipitation from July to September, presummer precipitation is more likely to be affected by local factors such as terrain and land cover. It has been reported that the amount and intensity of total precipitation in South China have increased due to the variation of large-scale circulation and climate change, such as increased surface temperature (Gemmer et al., 2011; Ren et al., 2015; Fu & Dan, 2014; Zhao et al., 2014; Fan et al., 2014). However, few studies have been focused on the variation in presummer precipitation and the effect of urbanization on presummer precipitation in South China.

In this study, we investigated and quantified the effect of urbanization on the variability of presummer precipitation in South China from 1979 to 2015, using a set of high-resolution gridded precipitation data and land cover data. The rest of the paper is organized as follows. Section 2 describes the data and methods applied in this study; the results and discussion are presented in section 3, following by the conclusions in section 4.

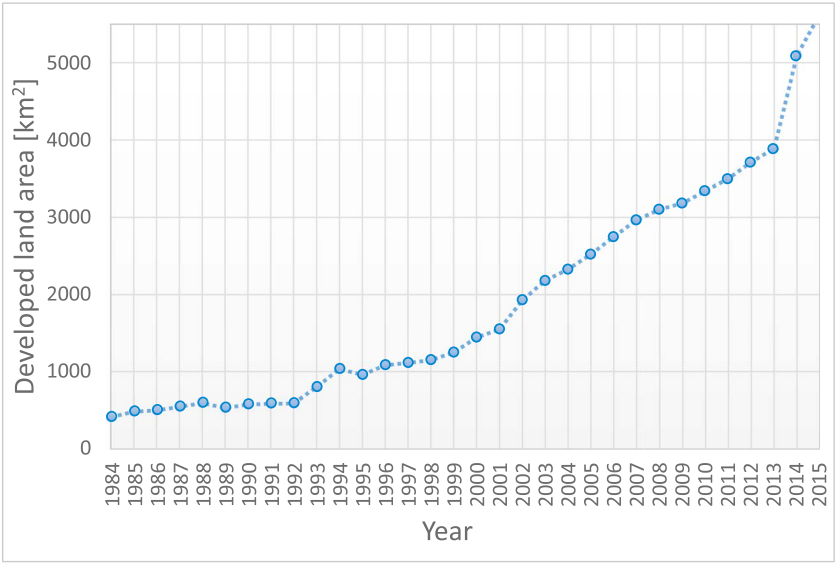

Figure 2. Time series of built urban areas of South China from 1984 to 2015.

2. Data and Methods

2.1. Data

2.1.1. CMFD

The China Meteorological Forcing Dataset (CMFD; Yang et al., 2010; Chen et al., 2011) is a reanalysis data set and developed by the hydrometeorological research group of the Institute of Tibetan Plateau Research of the Chinese Academy of Sciences. The data set was generated by merging the Princeton meteorological forcing data set (Sheffield et al., 2006), the Global Energy and Water Cycle Experiment-Surface Radiation Budget forcing data set (Pinker & Laszlo, 1992), the Global Land Data Assimilation System forcing data set (Rodell et al., 2004), precipitation data from the Tropical Rainfall Measuring Mission (Huffman et al., 2007; Huffman & Bolvin, 2013), and stationary observational meteorological data from the China Meteorological Administration. Dating from 1979, the CMFD contains 3-hourly gridded observations of near-surface temperature, pressure, wind speed and direction, specific humidity, surface precipitation rate, and surface downward shortwave and longwave radiation across China, with a spatial resolution of 0.1°.

2.1.2. Statistics on Developed Land Areas

There was very little developed land in South China in the 1980s, especially in the early 1980s (Zhu et al., 2011). According to the National Bureau of Statistics of China and the Bureau of Statistics of Guangdong, urban areas in GD grew slowly from 1984 to 1991, with developed land areas increasing from 413 to 588 km^2. However, the urban areas in GD have experienced an explosive expansion since 1992, with developed land increasing by a factor of 10, from 591 km^2 in 1992 to 5,633 km^2 in 2015 (Figure 2). The concentration of developed areas in the PRD has significantly altered the land surface properties of this region (Tse et al., 2018). In line with the evolution of development in South China, the period from 1979 to 2015 was divided into two parts in this study, the first from 1979 to 1991 and the second from 1992 to 2015, to quantify the difference in the variation of presummer precipitation in South China during these two periods and investigate the contribution of urbanization to the long-term variation in presummer precipitation in South China.

2.1.3. Satellite-Observed Land Cover Data

The European Space Agency launched the Climate Change Initiative (CCI) program in 2009 to provide high-quality satellite-derived products of essential climate variables, including land cover (Bontemps et al., 2013). The main objective of the CCI land cover project was to provide stable and comprehensive land cover data sets for the climate modeling community. The first phase of the CCI land cover generated the following set of products: three consistent global land cover data sets for the 1998–2002, 2003–2007, and 2008–2012 periods; 7-day time series representing the seasonal dynamics of the land surface; and medium-resolution imaging spectroradiometer surface reflectance time series, used as inputs to generate global land cover maps. The second phase of the project, which started in March 2014, generated a set of new and improved products: surface reflectance time series of Advanced Very High-Resolution Radiometer (AVHRR) global annual data and consistent land cover maps from 1992 to 2015 (Hansen et al., 2000).

Annual AVHRR land cover data with a spatial resolution of 300 m from 1992 to 2015 (Hansen et al., 1998) were used in this study to investigate the development of urbanization in South China during this period. Figure 3 shows the spatial distributions of urban areas in 1992, 2000, 2008, and 2015. The urban areas of South China are concentrated in the PRD and Shantou city on the east coast of GD. Since 1992, these areas have expanded rapidly, especially in the PRD, where the size of urban areas has increased considerably. This is consistent with the trend of urbanization reported by the National Bureau of Statistics of China and the Bureau of Statistics of Guangdong (Figure 2).

2.2. Methods

The trends of presummer precipitation in South China during the period from 1979 to 2015 were estimated and discussed. Presummer precipitation in South China indicates precipitation from 1 April to 30 June in this study, excluding precipitation caused by typhoons. Four indices were applied to describe the intensity of presummer precipitation in South China based on the gridded data in the CMFD. The definitions are listed in Table 1. Except for total precipitation during the presummer season (R), the indices were adopted to define extreme presummer precipitation, including maximum daily precipitation (R_{max}), very wet day precipitation (R_{95P}), and extremely heavy precipitation days with daily precipitation over 25 mm (R_{25mm}). Note that precipitation caused by typhoons was excluded.

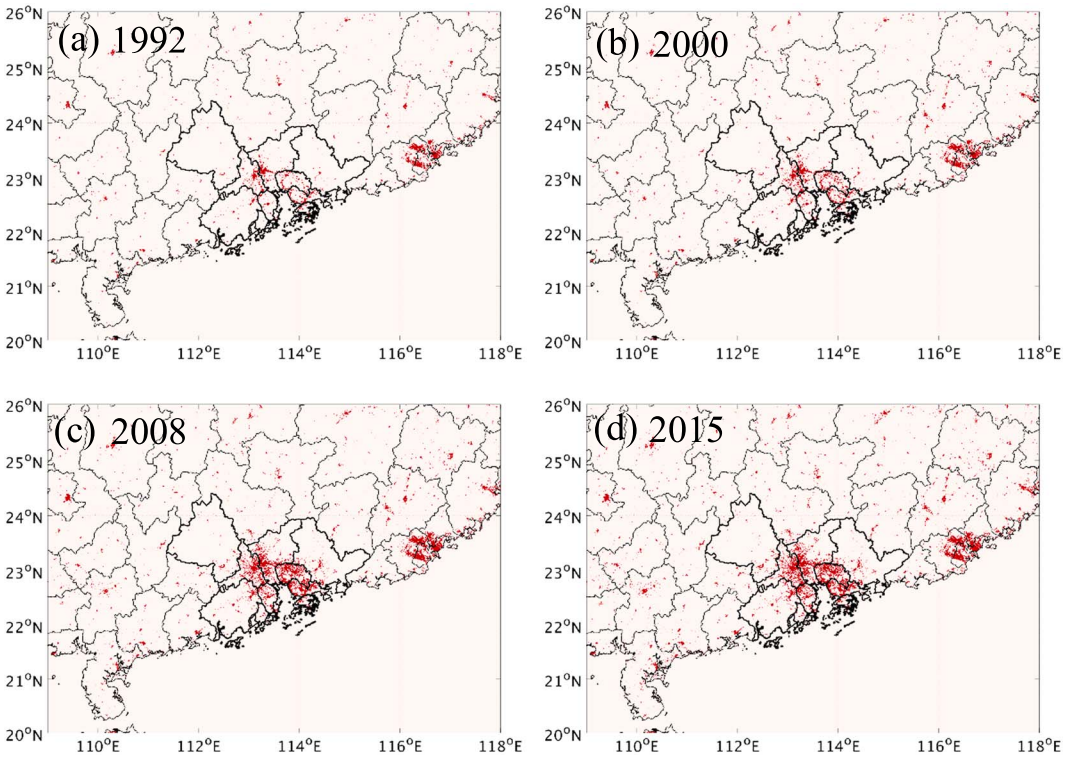

Figure 3. Urban area in South China at (a) 1992, (b) 2000, (c) 2008, and (d) 2015.

The Mann-Kendall test (Kendall, 1955) was applied for trend detection at each grid point. A trend was considered statistically significant if the probability of its occurrence by chance was less than 0.05. However, when n tests are performed simultaneously on a large quantity of data points at significance level of 0.05, the average number of tests for which the null is falsely rejected is $n \times 0.05$. For example, as we had 3,600 grid points over South China in the CMFD, testing for a trend in 3,600 locations where no change actually occurred would yield $3{,}600 \times 0.05$ (=180) significant locations on average, which was unacceptably high. Failure to correct multiple Mann-Kendall tests would lead to misidentification of the significance of the trends (Ventura et al., 2004). Therefore, a false discovery rate (FDR) procedure (Benjamini & Hochberg, 1995) was applied upon the multiple Mann-Kendall tests (hereafter the FDR-adjusted Mann-Kendall test) to adjust the significance level and control the proportion of falsely rejected null hypotheses relative to the total number of rejected hypotheses.

Furthermore, Sen's (1968) slope estimates were used to estimate linear trends during the investigated period for grid points that passed the FDR-adjusted Mann-Kendall test. In addition to the trends of individual data grids, the mean trends in urban and nonurban areas were calculated by averaging the time series of presummer precipitation in specific areas to assess the contribution of urbanization to the variation of presummer precipitation.

Table 1
Definition of Precipitation Indices Used in This Study

Index	Descriptive name	Definition	Unit
R	Total presummer precipitation	Total precipitation during presummer season	mm
R_{max}	Maximum daily precipitation	Maximum daily precipitation during presummer season	mm/day
R_{95P}	Very wet day precipitation	Total precipitation when daily precipitation >95th percentile mean daily precipitation during presummer season	mm
R_{25mm}	Extremely heavy precipitation days	Count of days with daily precipitation ≥25 mm during presummer season	days

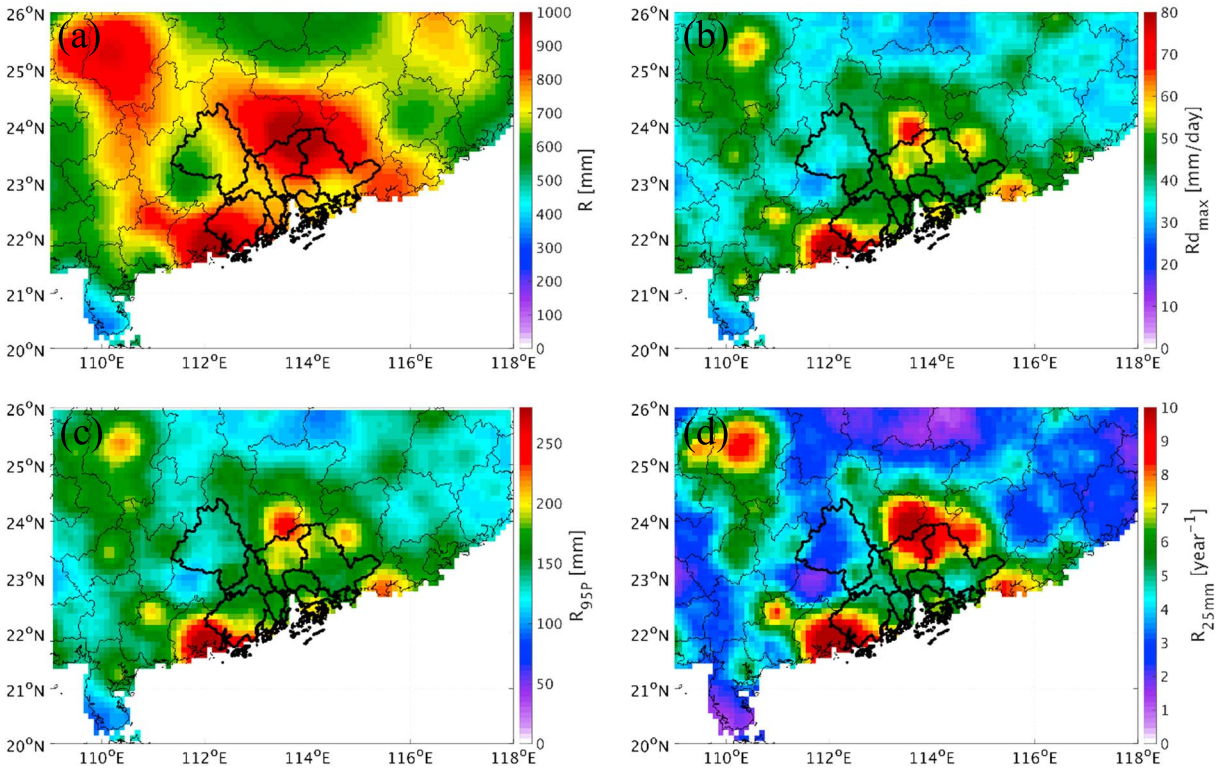

Figure 4. Spatial distribution of mean (a) R, (b) R_{max}, (c) R_{95P}, and (d) R_{25mm} over South China during presummer season from 1979 to 2015.

3. Results and Discussion

3.1. Spatial Distributions of Presummer Precipitation in South China

Figure 4 shows the spatial distributions of presummer precipitation in South China based on the four indices listed in Table 1.

The annual mean R in South China from 1979 to 2015 ranged from 300 mm to over 1,000 mm, accounting for 30–70% of annual total precipitation (Figure 4a). There are three precipitation maxima in South China during the presummer season. The highest precipitation maximum is on the southwestern coast of GD, the maximum located northeast of the PRD region is slightly lower, and the lowest precipitation maximum is in the northwest of South China. The main cause of precipitation maxima is likely related to local terrain. As Figure 1 shows, the three precipitation maxima are located on the southern slopes of the mountains, supporting the development of convection due to terrain-induced lift. The release of latent heat by moisture condensation further enhances the convective system, leading to stronger precipitation.

The annual mean R_{max} in South China during the presummer season from 1979 to 2015 ranged from 20 mm to over 80 mm (Figure 4b), and the mean R_{95P} ranged from 10 mm to over 50 mm (Figure 4c). Their spatial distributions are similar, with one maximum located on the southwestern coast of GD and the other located northeast of the PRD.

The annual mean R_{25mm} from 1979 to 2015 ranged from 1 to more than 10 days/year on average (Figure 4d). The maximum values located at the two precipitation maxima on the southwestern coast of GD and northeast of the PRD, with a mean R_{25mm} of 12 days/year, indicating 12 occurrences of extremely heavy precipitation during the presummer season each year.

3.2. Spatiotemporal Variability of Presummer Precipitation in South China

The FDR-adjusted Mann-Kendall test was applied to the four presummer precipitation indices, R, R_{max}, R_{95P}, and R_{25mm}, at each grid point in South China to detect whether there existed a significant trend during the period from 1979 to 2015. In addition, the linear trends of each index were calculated in the grids that

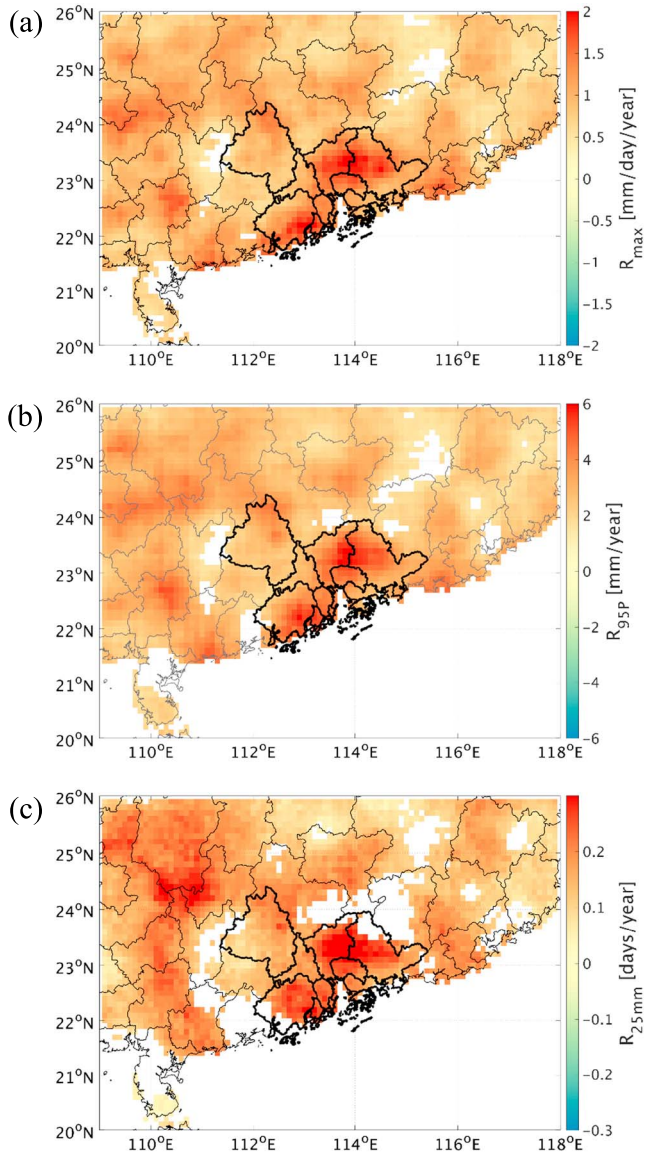

Figure 5. Spatial distributions of linear trends of (a) R_{max}, (b) R_{95P}, and (c) R_{25mm} over South China during presummer season from 1979 to 2015.

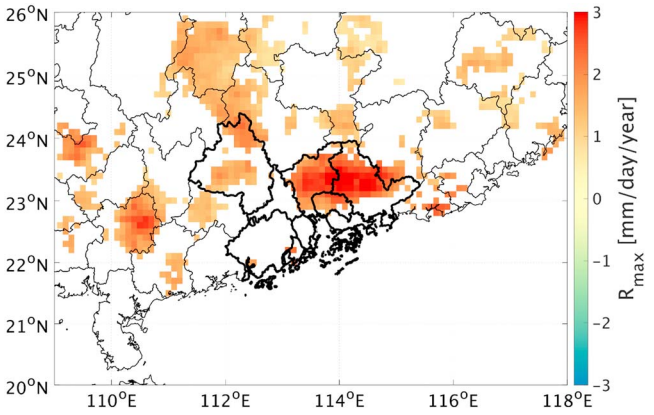

Figure 6. Spatial distributions of linear trend of R_{max} over South China during presummer season from 1992 to 2015.

passed the test. As urbanization in South China has increased rapidly since 1992, we further divided the period from 1979 to 2015 into two parts, one from 1979 to 1991 and the other from 1992 to 2015, and applied the procedures described above to obtain the trends of the four indices for each part.

3.2.1. Spatial Distributions of Trends of Presummer Precipitation

The spatial distributions of the linear trends of presummer precipitation in South China from 1979 to 2015 are shown in Figure 5. As R shows no significant trend in South China during the period from 1979 to 2015, only the spatial distributions of R_{max}, R_{95P}, and R_{25mm} are presented. Note that only grids with trends that pass the FDR-adjusted Mann-Kendall test at a significance level of 0.05 are shown in Figure 5. In addition, the PRD region is highlighted by solid lines on the map.

The spatial distributions of the linear trends of R_{max} (Figure 5a), R_{95P} (Figure 5b), and R_{25mm} (Figure 5c) are similar, with significant upward trends throughout South China from 1979 to 2015. The fastest increase is located in the northeastern part and west coast of the PRD, with a rate of up to 3 mm/year. This increasing rate indicates that the maximum daily precipitation during the presummer season increased by more than 100 mm from 1979 to 2015, whereas the mean R_{max} in the region is only between 50 and 100 mm during the period, as shown in Figure 4b.

The increasing rate of R_{95P} reached 6 mm/year in the northeastern part and west coast of the PRD (Figure 5b); that is, the total amount of the top 5% daily precipitation during the presummer season increased by approximately 220 mm from 1979 to 2015, which is greater than the mean R_{95P} (150–200 mm) in the region during the period (Figure 4c).

R_{25mm} shows an increasing rate of up to over 0.4 mm/year in the northeastern part of the PRD (Figure 5c). As a result, the number of extremely heavy precipitation days increased by more than 15 days from 1979 to 2015, indicating a doubling of the number of extremely heavy precipitation days in the region during the period.

As previously mentioned, as the urbanization over South China speeded up since 1992, we divided the investigated period into two parts, one from 1979 to 1992 and the other from 1992 to 2015. The trends of presummer precipitation in South China for the two periods were calculated separately. As no grid points passed the FDR-adjusted Man-Kendall test for the period from 1979 to 1992 for the four indices, the trends of presummer precipitation are statistically insignificant throughout South China during this period and are thus not presented here. For the period from 1992 to 2015, however, R_{max} shows substantial upward trends in parts of South China, especially in the northeastern part of the PRD, as shown in Figure 6. The increasing rate reaches more than 3 mm/day/year, indicating an increase of 72 mm in maximum daily precipitation during the presummer season, which accounts for 80% to 100% of the mean maximum daily precipitation in the region during the period.

In summary, the intensity of precipitation and the number of extremely heavy precipitation days during presummer season in South China have significantly increased from 1979 to 2015, especially in the central PRD. In addition, the increase in the maximum daily precipitation is much faster during the period from 1992 to 2015 than that from 1979 to 1991, accompanying the acceleration of the urbanization of the PRD.

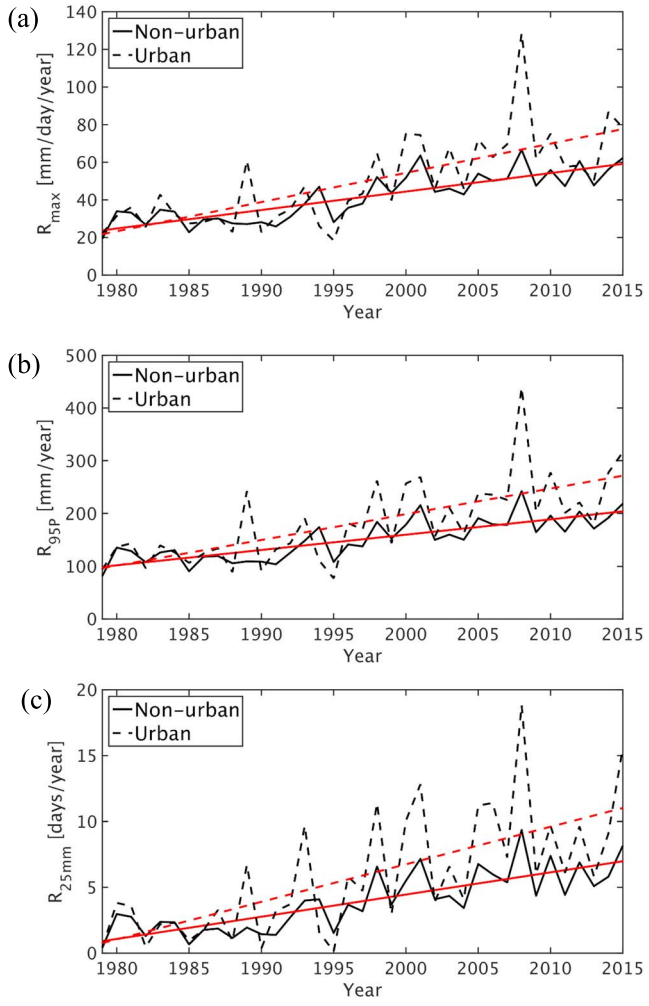

Figure 7. Mean trends of presummer (a) R_{max}, (b) R_{95P}, and (c) R_{25mm} over urban (dash lines) and nonurban (solid lines) areas of South China during the period from 1979 to 2015.

3.2.2. Mean Trends of Presummer Precipitation in South China

To further investigate the trends of presummer precipitation in urban and nonurban areas, we divided South China into urban and nonurban areas according to AVHRR land cover maps. Specifically, the AVHRR land cover map for 2015 was then applied to divide South China into urban and nonurban areas (Figure 3a).

The 300-m-resolution land cover map was regridded into a 0.1° map according to the spatial resolution of the CMFD data set. For each grid of the new land cover map, if the original urban grid accounts for over 50% of the total area of the new grid, it was defined as an urban grid; otherwise, it was defined as a nonurban grid. For each precipitation index considered in this study, the FDR-adjusted Mann-Kendall test was applied to each grid of urban and nonurban areas to detect whether there was a significant trend during the period from 1979 to 2015. Only those grids that passed the test at a significance level of 0.05 (as shown in Figures 5) were selected for the calculation of the mean trends. The indices were then spatially averaged in the selected grids of urban and nonurban areas, and the trends of each index were calculated based on the spatial means of this index in urban and nonurban areas for the periods from 1979 to 1992, 1992 to 2015, and 1979 to 2015. As mentioned in the previous section, no data grid passed the FDR-adjusted Mann-Kendall test for R, indicating that the total amount of presummer precipitation shows no significant trend from 1979 to 2015. Therefore, only the mean trends of R_{max}, R_{95P}, and R_{25mm} are presented and discussed in this section.

Figure 7 shows the mean trends of R_{max}, R_{95P}, and R_{25mm} during the investigated period from 1979 to 2015. The trends are all significant at a significance level of 0.01. Although the three indices exhibit consistent upward trends in both urban and nonurban areas, the trends in urban areas are significantly higher than those in nonurban areas. The mean R_{max} in urban and nonurban areas have approximate values for the first years of the investigated period but began to show an upward trend after 1992. R_{95P} and R_{25mm} show similar results. This transition is likely related to the long-term variations in presummer precipitation in South China, such as decadal oscillations. However, it is important to note that the discrepancies between urban and nonurban areas widen over time, leading to much more significant upward trends for R_{max}, R_{95P}, and R_{25mm} in urban areas than nonurban areas after 1992.

As shown in Figure 8a, after dividing the investigated period into two parts before and after 1992, R_{max} shows a slight decrease in nonurban areas and a slight increase in urban areas from 1979 to 1991, with trends of −0.36 and 0.21 mm/day/year (Table 2), respectively. Neither is statistically significant. In contrast, R_{max} shows an increase in both urban and nonurban areas from 1992 to 2015, with trends of 1.70 mm/day/year in urban areas and 0.96 mm/day/year in nonurban areas (Table 2), significant at a confidence level of 0.05 and 0.01, respectively. In other words, the maximum daily precipitation during the presummer season has increased by 40.80 and 23.04 mm/day on average in urban and nonurban areas, respectively, from 1992 to 2015. For the whole investigated period from 1979 to 2015, the mean trends of R_{max} are 1.34 and 0.97 mm/day/year in urban and nonurban areas, respectively, and both are significant at a significance level of 0.01, indicating an average increase of 49.58 and 35.89 mm/day for maximum daily precipitation during the presummer season in urban and nonurban areas, respectively.

Similarly, in Figure 8b, R_{95P} shows an insignificant decrease in nonurban areas and an insignificant increase in urban areas from 1979 to 1991. However, an increase can be seen in both urban and nonurban areas from 1992 to 2015, with mean trends of 5.39 and 2.61 mm/year, respectively; both are significant at a significance level of 0.01 (Table 2). As a result, the top 5% of daily precipitation during the presummer season has increased by 129.36 and 62.64 mm on average in urban and nonurban areas, respectively. For the whole

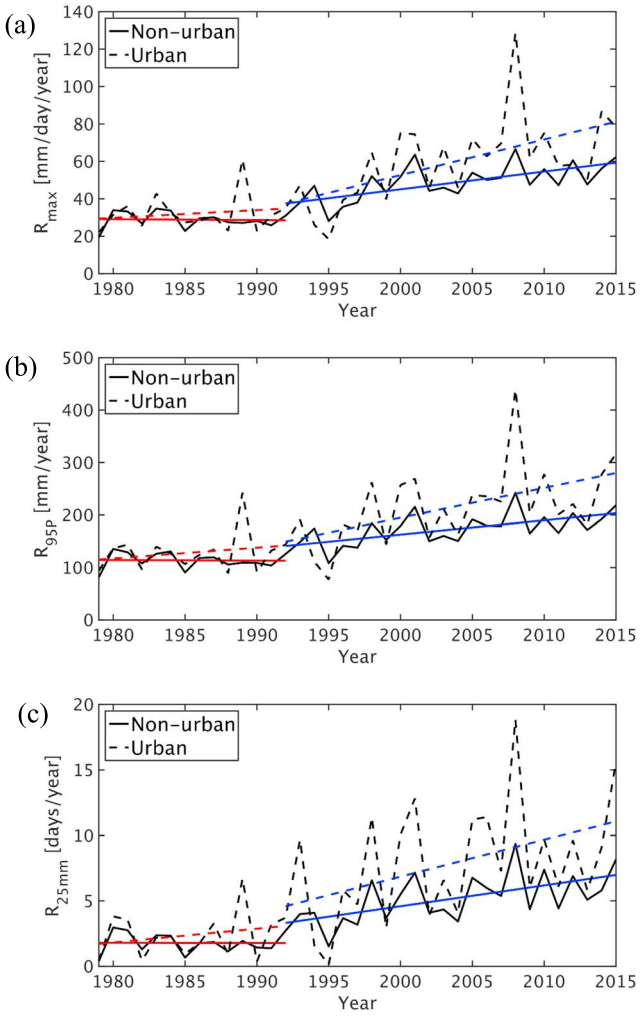

Figure 8. Mean trends of presummer (a) R_{max}, (b) R_{95P}, and (c) R_{25mm} over urban (dash lines) and nonurban (solid lines) areas of South China during the period from 1979 to 1991 and 1992 to 2015.

investigated period from 1979 to 2015, the mean trends of R_{95P} are 4.41 and 2.79 mm/year in urban and nonurban areas, respectively, both are significant at a significance level of 0.01 (Table 2). This leads to an average increase of 163.17 and 103.23 mm for the top 5% of daily precipitation during the presummer season in urban and nonurban areas, respectively.

In Figure 8c, R_{25mm} also shows a slight decrease in nonurban areas and a slight increase in urban areas from 1979 to 1991, although neither is statistically significant. In contrast, R_{25mm} shows a significant increase from 1992 to 2015 in both urban and nonurban areas, with mean trends of 0.26 and 0.15 days/year (Table 2), suggesting an average increase of 6.24 and 3.60 days of extremely heavy precipitation during the presummer season in urban and nonurban areas, respectively. For the whole investigated period from 1979 to 2015, the mean trends of R_{25mm} are 0.26 and 0.16 days/year in urban and nonurban areas, both are significant at a significance level of 0.01 (Table 2), indicating that the number of extremely heavy precipitation days during the presummer season has increased by 9.62 and 5.92 days in urban and nonurban areas, respectively.

In summary, although the total amount of presummer precipitation shows no significant trend in South China, the intensity of precipitation and the number of extremely heavy precipitation events during the presummer season have increased significantly throughout South China from 1979 to 2015. This increase can be attributed to the change in presummer precipitation since 1992, which is likely related to a long-term variation of presummer precipitation, such as decadal oscillations. However, the upward trends of presummer precipitation are much higher in urban areas than nonurban areas, suggesting that the explosive urbanization has contributed to the intensification of presummer precipitation and the increase of extremely heavy precipitation events during the presummer season in urban areas of South China.

3.3. Discussion

3.3.1. Sensitivity of Mean Trends to "Urban Areas" of Different Years

As reported in section 3.2.2, the AVHRR land cover map of 2015 was used to identify urban and nonurban grids to investigate the discrepancies between the trends of presummer precipitation in urban and nonurban areas of South China during the period from 1979 to 2015. However, this classification may include some "urban grids" gradually converted from nonurban grids during the period from 1992 to 2015. In this case, the calculated trends for urban areas could include an effect of nonurban areas. On the other hand, there was little increase in urban areas in South China before 1992 according to Figure 2. Therefore, we assumed that the urban areas of South China in 1979 were similar to those in 1992, meaning that the identified urban grids based on the land cover data of 1992 should be urban throughout the entire investigated period, from 1979 to 2015. To better understand the effect of "nonurban grids" transformed into urban grids on the trends of presummer precipitation in South China during the period from 1992 to 2015, we ran a sensitivity test by using the AVHRR land cover map of 1992, 2000, and 2008 shown in Figures 3a, 3b, and 3c to classify urban and nonurban grids in the same method as described in section 3.2.2 and calculated the respective mean trends in urban and nonurban areas. The mean trends for each index of presummer precipitation are summarized in Table 2. Note that for 1992, there was no mean trends for all indices of presummer precipitation in urban area of South China, as no grid passed the FDR-adjusted Mann-Kendall test in urban areas when we applied the criterion that a grid was identified as an urban grid if the original urban grid accounted for more than 50% of the total area of the new grid. Therefore, we ran an extra test for 1992 by applying a lower criterion according to which a grid was classified as an urban grid if the original urban grid accounted for more than 30% of the total area of the new grid.

Table 2
Mean Trend of Presummer Precipitation and Daily Mean Temperature From 1979 to 2015 Over Grids Passed False Discovery Rate-Adjusted Mann-Kendall Test

Land cover map/criterion for urban grids	Period	R_{max} (mm/day/year)		R_{95P} (mm/year)		R_{25mm} (days/year)		Temp (°C/year)	
		Nonurban	Urban	Nonurban	Urban	Nonurban	Urban	Nonurban	Urban
1992/30%	1979–1992	−0.36	0.19	−0.81	0.97	−0.02	0.06	0.02	0.03
	1992–2015	0.96**	1.65*	2.61**	4.64**	0.15**	0.27*	0.02	0.03
	1979–2015	0.97**	1.34**	2.79**	4.35**	0.16**	0.23**	0.03**	0.05**
1992/50%	1979–1992	−0.36	—	−0.81	—	−0.02	—	0.02	—
	1992–2015	0.96**	—	2.61**	—	0.15*	—	0.02	—
	1979–2015	0.97**	—	2.79**	—	0.15**	—	0.03	—
2000/50%	1979–1992	−0.36	0.22	−0.81	—	−0.02	—	0.02	—
	1992–2015	0.96**	1.56*	2.61**	—	0.15**	—	0.02	—
	1979–2015	0.97**	1.35**	2.78**	—	0.16**	—	0.03**	—
2008/50%	1979–1992	−0.36	0.23	−0.81	−0.31	−0.02	0.10	0.02	0.03
	1992–2015	0.96**	1.69*	2.61**	5.49*	0.15*	0.27*	0.02	0.03
	1979–2015	0.97**	1.35**	2.79**	4.44**	0.16**	0.27**	0.03**	0.05**
2015/50%	1979–1992	−0.36	0.21	−0.81	0.80	−0.02	0.09	0.02	0.03
	1992–2015	0.96**	1.70*	2.61**	5.39**	0.15**	0.26*	0.02	0.03
	1979–2015	0.97**	1.34**	2.79**	4.41**	0.16**	0.26**	0.03**	0.05**

Note. Em dash (—) means there is no valid grid for calculating the mean trend.
*A trend significant at significance level of 0.05. **A trend significant at significance level of 0.01.

Generally, the mean trends of R_{max}, R_{95P}, and R_{25mm} remain almost the same in nonurban areas with the different land cover maps from 2015 to 1992. However, the mean trends in urban areas show slight differences with the different land cover map from 2015 to 1992. For instance, applying the land cover data of 2008 and 2000, the mean trends of R_{max} is 1.69 and 1.56 mm/day/year, respectively, during the period from 1992 to 2015, 0.01 and 0.14 mm/day/year lower than the trend obtained using the land cover date of 2015. The mean trend of R_{95P} is 5.49 mm/year for the period from 1992 to 2015 with the land cover data of 2008, 0.10 mm/year higher than that obtained with the land cover data of 2015. One reason may be that the number of urban grids is much smaller than the number of nonurban grids in the region studied. As a result, the effect of a few urban grids transformed into nonurban grids can be much greater on urban areas than on nonurban areas. The other reason may be that by using an older land cover map, it excludes the effect of nonurban grids recently transformed into urban grids but recognized as urban grids by using a recent land cover map. However, the differences in mean trends induced by applying the land cover maps of different years are not significant, the mean trends of presummer precipitation remaining almost the same in nonurban and urban areas for the period from 1979 to 2015, even when we lowered the criterion for selecting urban grids when using the land cover map of 1992.

In addition, the mean trends for the four indices over all grids of South China are shown in Table 3. Compared with the mean trends of grids that passed the FDR-adjusted Mann-Kendall test, the mean trends over all grids are consistently smaller. Nevertheless, the mean trends in urban areas are significantly higher than those in nonurban area for the four indices.

Table 3
Mean Trend of Presummer Precipitation and Daily Mean Temperature From 1979 to 2015 Over All Grids

Region	R (mm/year)		R_{max} (mm/day/year)		R_{95P} (mm/year)		R_{25mm} (days/year)		T_{emp} (°C/year)	
	Nonurban	Urban	Nonurban	Urban	Nonurban	Urban	Nonurban	Urban	Nonurban	Urban
1979–1991	−5.01	−1.72	−0.02	0.24	−0.26	0.86	0.00	0.00	0.01	0.04
1992–2015	0.72	5.28	0.75**	1.20*	1.91**	3.88*	0.02*	0.05*	0.02	0.01
1979–2015	1.60	3.88	0.66**	1.00**	1.89**	3.05**	0.02**	0.04**	0.03**	0.04**

*A trend significant at significance level of 0.05. **A trend significant at significance level of 0.01.

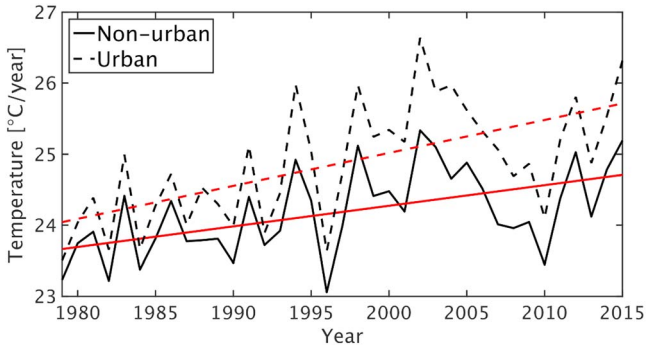

Figure 9. Mean trends of daily mean temperature over urban (dash lines) and nonurban (solid lines) areas of South China during presummer season from 1979 to 2015.

3.3.2. Effect of Urbanization on Presummer Precipitation

The consistent upward trends in the intensity of precipitation and the number of extremely heavy precipitation days during the presummer season in both urban and nonurban areas from 1979 to 2015 suggest that changes in large-scale atmospheric circulation are likely to be the main cause of the variation in precipitation patterns. However, the significant discrepancies between the trends in urban and nonurban areas indicate a significant effect of urbanization on the variability of extreme precipitation during the presummer season in South China.

As shown in Table 2, although the mean trends of R_{max}, R_{95P}, and R_{25mm} are not significant in both urban and nonurban areas from 1979 to 1991, the trends of the three indices in urban areas are different from those in nonurban area. Furthermore, the upward trends of R_{max}, R_{95P}, and R_{25mm} in urban areas are, respectively, between 62.50% and 77.08%, 106.51% and 137.14%, and 73.33% and 80.00% higher than over nonurban area for the period from 1992 to 2015. Moreover, for the whole investigated period from 1979 to 2015, the upward trends of R_{max}, R_{95P}, and R_{25mm} in urban areas are, respectively, between 38.14% and 39.18%, 55.97% and 59.14%, and 43.75% and 68.75% higher than in nonurban areas, which can be attributed to the urban effect on the intensity of presummer precipitation and the occurrence of extremely heavy precipitation during the presummer season in South China.

The urban heat island effect may be one factor influencing the urban effect on presummer precipitation in South China. On average, the mean surface temperature in urban areas is 1.11 °C higher than that in nonurban area for the period from 1979 to 2015 (Figure 9), and the mean trend of surface temperature in urban areas is 0.05 °C/year during the period from 1979 to 2015, 0.02°C/year higher than that in nonurban area (Table 2). Urban heat islands may act as a low-level heat source in urban areas and provide extra energy to induce vertical flows and enhance convective motion, leading to more convective precipitation in urban and downwind areas (Craig, 2002; Rozoff et al., 2003; Shem & Shepherd, 2009; Lin et al., 2011). Strong convective motion is the main cause of extreme precipitation during the presummer season in South China. As Figure 10 shows, the upward trend of surface temperature in the PRD is the most significant on the west coast of the PRD, which is one of the areas with the fastest increasing trends of R_{max} (Figure 5a), R_{95P} (Figure 5b), and R_{25mm} (Figure 5c) throughout the investigated period.

In addition, urbanization modifies surface properties, which can also affect vertical flows in urban areas. Due to larger surface roughness, air masses approaching a cluster of cities tend to slow down. This is illustrated in Figure 11, in which the annual mean wind speed from the CMFD shows an overall decrease over west and east coasts of the Pearl River estuary during the period from 1979 to 2015. The blocked air masses then divert in front of the cities and converge at the downwind areas, resulting in upward motions (Cotton & Pielke, 2007). Furthermore, there are more and more high-rise buildings in urban areas of South China, especially in the PRD, resulting in a higher surface elevation. This surface elevation forces the approaching moist air masses to rise, leading to stronger upward motions, and thus, more moist convections are initiated. During the presummer season, a large amount of moisture is transported to South China typically by southerly and southwesterly winds, resulting in strong moist convection and intense precipitation when encountering frontal systems. In Figure 11, the downward trend of wind speed extends from the coast of the Pearl River estuary to the northwest part of the PRD, leading to a convergence of moisture and an accumulation of thermal energy in the northeast part of the PRD when southerly or southwesterly winds prevails. In such cases, the moist convections can be enhanced by the dense high-rising buildings in cities surrounding the Pearl River estuary, resulting in stronger precipitations

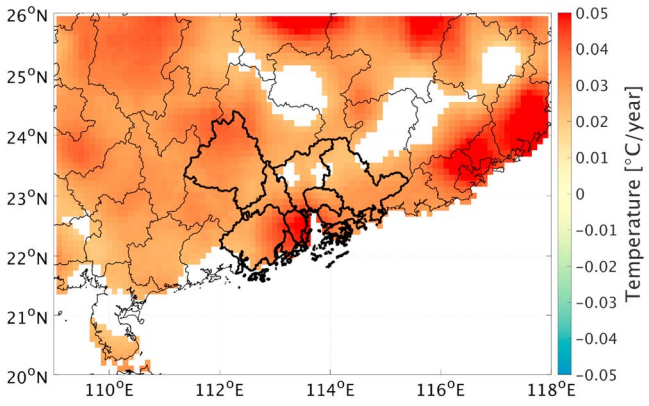

Figure 10. Spatial distribution of linear trends of mean temperature over South China during presummer season from 1979 to 2015.

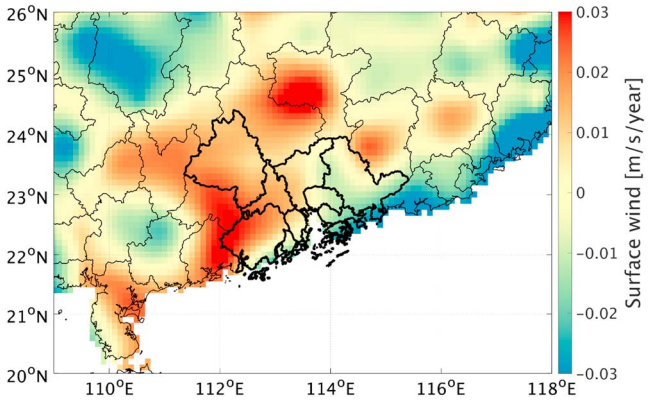

Figure 11. Spatial distribution of linear trends of mean surface wind speed over South China during presummer season from 1979 to 2015.

in the adjacent downstream areas, the northeast part of the PRD, leading to the most significant trends of R_{max} (Figure 5a), R_{95P} (Figure 5b), and R_{25mm} (Figure 5c) in this area.

4. Summary

The variation in presummer precipitation in South China from 1979 to 2015 and its relationship with urbanization were analyzed in this study. The results reveal that the intensity of precipitation and the number of extremely heavy precipitation days during the presummer season have increased significantly throughout South China, and the upward trend is much more significant in urban areas than in nonurban areas.

The total amount of presummer precipitation shows no significant trend, in urban and nonurban areas of South China. However, the mean trends in urban and nonurban areas are, respectively, 1.34 and 0.97 mm/day/year for maximum daily precipitation, 4.41and 2.79 mm/year for the top 5% of daily precipitation, and 0.26 and 0.16 days/year for extremely heavy precipitation days with daily precipitation greater than 25 mm during the presummer season in South China.

The consistent trends of presummer precipitation in urban and nonurban areas from 1979 to 2015 indicate that changes in large-scale atmospheric circulation are likely the main reason for the variation in precipitation during the presummer season in South China. However, the significant discrepancies between the trends in urban and nonurban areas, especially during the rapid growth of urban areas from 1992 to 2015, suggest a significant effect of urbanization on the total amount and intensity of precipitation and the occurrence of extremely heavy precipitation during the presummer season in South China. The upward trends of maximum daily precipitation, the top 5% of daily precipitation, and extremely heavy precipitation days in urban areas are, respectively, between 38.14% and 39.18%, 55.97% and 59.14%, and 43.75% and 68.75% higher than those in nonurban areas for the entire investigated period. In contrast, the upward trends of maximum daily precipitation, the top 5% of daily precipitation, and extremely heavy precipitation days in urban areas are, respectively, between 62.50% and 77.08%, 106.51% and 137.14%, and 73.33% and 80.00% higher than those in nonurban areas during the period from 1992 to 2015. These discrepancies between urban and nonurban areas can be attributed to the effect of urbanization on presummer precipitation in South China.

The results of this study suggest that in addition to the variability of large-scale variation, urbanization seems to play an important role to enhance local precipitation and accelerating the intensification of local extreme precipitation in the presummer season in South China in recent decades. The distributions of the trends of presummer precipitation in South China further indicate that the increased intensification of presummer precipitation in urban area is related to a faster upward trend in surface temperature, higher surface roughness, and higher density of high-rise buildings in urban areas. Therefore, urban areas in South China will face a greater threat of extreme precipitation than nonurban areas in the presummer season in the course of global warming.

Acknowledgments

We are deeply grateful to the principal investigators and their staff at the Data Assimilation and Modeling Centre for Tibetan Multi-spheres, Institute of Tibetan Plateau Research, Chinese Academy of Sciences for the provision of the CMFD used in this study. The data set is available online (http://westdc.westgis.ac.cn/data/7a35329c-c53f-4267-aa07-e0037d913a21). We would like to thank the principal investigators and their staff at the Global Land Cover Facility of the University of Maryland for providing the global land cover classification dataset derived from the AVHRR. We would also like to thank the anonymous reviewers of this manuscript for their constructive comments and suggestions that led to the improvement of this work. The land cover data can be accessed online (http://maps.elie.ucl.ac.be/CCI/viewer/). All of the data used in this paper are cited and referred to in the reference list. This work was supported by the RGC Grants 16303416 and AoE/E-603/18 and the National Air pollution Control Program of the National Key Research & Development Plan 2018YFC0213902.

References

Allan, R. P., & Soden, B. J. (2008). Atmospheric warming and the amplification of precipitation extremes. *Science*, *321*(5895), 1481–1484. https://doi.org/10.1126/science.1160787

Baik, J.-J. (1992). Response of a stably stratified atmosphere to low-level heating—An application to the heat island problem. *Journal of Applied Meteorology*, *31*(3), 291–303. https://doi.org/10.1175/1520-0450(1992)031<0291:ROASSA>2.0.CO;2

Benjamini, Y., & Hochberg, Y. (1995). Controlling the false discovery rate: A practical and powerful approach to multiple testing. *Journal of the Royal Statistical Society: Series B (Methodological)*, *57*, 289–300.

Bontemps, S., Defourny, P., Radoux, J., Van Bogaert, E., Lamarche, C., Achard, F., et al., 2013 Consistent global land cover maps for climate modelling communities: Current achievements of the ESA's land cover CCI, Proceedings of the ESA Living Planet Symposium.

Bornstein, R., and LeRoy, M.: Urban barrier effects on convective and frontal thunderstorms, Extended Abstracts, Fourth Conf. on Mesoscale Processes, 1990, 120-121.

Chen, T.-C., Huang, W.-R., & Yen, M.-C. (2011). Interannual variation of the late spring–early summer monsoon rainfall in the northern part of the South China Sea. *Journal of Climate*, *24*(16), 4295–4313. https://doi.org/10.1175/2011JCLI3930.1

Chen, Y., Yang, K., He, J., Qin, J., Shi, J., Du, J., & He, Q. (2011). Improving land surface temperature modeling for dry land of China. *Journal of Geophysical Research*, *116*, D20104. https://doi.org/10.1029/2011JD015921

Cotton, W. R., & Pielke, R. A. Sr. (2007). *Human impacts on weather and climate*. Cambridge University Press. https://doi.org/10.1017/CBO9780511808319

Craig, K. J.: MM5 Simulations of urban induced convective precipitation over Atlanta, GA, 2002.

Fan, K., Xu, Z., & Tian, B. (2014). Has the intensity of the interannual variability in summer rainfall over South China remarkably increased? *Meteorology and Atmospheric Physics*, *124*(1-2), 23–32. https://doi.org/10.1007/s00703-013-0301-5

Fu, C., & Dan, L. (2014). Trends in the different grades of precipitation over South China during 1960–2010 and the possible link with anthropogenic aerosols. *Advances in Atmospheric Sciences*, *31*(2), 480–491. https://doi.org/10.1007/s00376-013-2102-7

Gemmer, M., Fischer, T., Jiang, T., Su, B., & Liu, L. L. (2011). Trends in precipitation extremes in the Zhujiang River basin, South China. *Journal of climate*, *24*(3), 750–761. https://doi.org/10.1175/2010JCLI3717.1

Han, J.-Y., & Baik, J.-J. (2008). A theoretical and numerical study of urban heat island–induced circulation and convection. *Journal of the Atmospheric Sciences*, *65*(6), 1859–1877. https://doi.org/10.1175/2007JAS2326.1

Hansen, M., R. DeFries, J.R.G. Townshend, and R. Sohlberg (1998), UMD Global Land Cover Classification, 1 Kilometer, 1.0, Department of Geography, University of Maryland, College Park, Maryland, 1981-1994.

Hansen, M. C., DeFries, R. S., Townshend, J. R., & Sohlberg, R. (2000). Global land cover classification at 1 km spatial resolution using a classification tree approach. *International journal of remote sensing*, *21*(6-7), 1331–1364. https://doi.org/10.1080/014311600210209

Huang, S. S. (1986). *The heavy rain during the pre-summer period over Southern China (in Chinese)* (p. 244). Guangdong Technology Press.

Huff, F., & Changnon, S. Jr. (1973). Precipitation modification by major urban areas. *Bulletin of the American Meteorological Society*, *54*(12), 1220–1232. https://doi.org/10.1175/1520-0477(1973)054<1220:PMBMUA>2.0.CO;2

Huffman, G. J., and Bolvin, D. T.: TRMM and other data precipitation data set documentation, NASA, Greenbelt, USA, 28, 2013.

Huffman, G. J., Bolvin, D. T., Nelkin, E. J., Wolff, D. B., Adler, R. F., Gu, G., et al. (2007). The TRMM multisatellite precipitation analysis (TMPA): Quasi-global, multiyear, combined-sensor precipitation estimates at fine scales. *Journal of hydrometeorology*, *8*(1), 38–55. https://doi.org/10.1175/JHM560.1

Kendall, M. G.: Rank correlation methods, 1955.

Kunkel, K. E., Andsager, K., & Easterling, D. R. (1999). Long-term trends in extreme precipitation events over the conterminous United States and Canada. *Journal of climate*, *12*(8), 2515–2527. https://doi.org/10.1175/1520-0442(1999)012<2515:LTTIEP>2.0.CO;2

Li, Z., Yan, Z., Tu, K., & Wu, H. (2015). Changes of precipitation and extremes and the possible effect of urbanization in the Beijing metropolitan region during 1960–2012 based on homogenized observations. *Advances in Atmospheric Sciences*, *32*(9), 1173–1185. https://doi.org/10.1007/s00376-015-4257-x

Liang, P., & Ding, Y. (2017). The long-term variation of extreme heavy precipitation and its link to urbanization effects in Shanghai during 1916–2014. *Advances in Atmospheric Sciences*, *34*(3), 321–334. https://doi.org/10.1007/s00376-016-6120-0

Lin, C.-Y., Chen, W.-C., Chang, P.-L., & Sheng, Y.-F. (2011). Impact of the urban heat island effect on precipitation over a complex geographic environment in northern Taiwan. *Journal of Applied Meteorology and Climatology*, *50*(2), 339–353. https://doi.org/10.1175/2010JAMC2504.1

Madsen, H., Lawrence, D., Lang, M., Martinkova, M., & Kjeldsen, T. (2014). Review of trend analysis and climate change projections of extreme precipitation and floods in Europe. *Journal of Hydrology*, *519*, 3634–3650. https://doi.org/10.1016/j.jhydrol.2014.11.003

Niyogi, D., Lei, M., Kishtawal, C., Schmid, P., & Shepherd, M. (2017). Urbanization impacts on the summer heavy rainfall climatology over the eastern United States. *Earth Interactions*, *21*, 1–17.

Pinker, R., & Laszlo, I. (1992). Modeling surface solar irradiance for satellite applications on a global scale. *Journal of Applied Meteorology*, *31*(2), 194–211. https://doi.org/10.1175/1520-0450(1992)031<0194:MSSIFS>2.0.CO;2

Qiang, X. M., & Yang, X. Q. (2008). Onset and end of the first rainy season in South China. *Chinese Journal of Geophysics*, *51*(5), 944–957. https://doi.org/10.1002/cjg2.1289

Ren, Z., Zhang, M., Wang, S., Qiang, F., Zhu, X., & Dong, L. (2015). Changes in daily extreme precipitation events in South China from 1961 to 2011. *Journal of Geographical Sciences*, *25*(1), 58–68. https://doi.org/10.1007/s11442-015-1153-3

Rodell, M., Houser, P., Jambor, U., Gottschalck, J., Mitchell, K., Meng, C., et al. (2004). The global land data assimilation system. *Bulletin of the American Meteorological Society*, *85*(3), 381–394. https://doi.org/10.1175/BAMS-85-3-381

Rozoff, C. M., Cotton, W. R., & Adegoke, J. O. (2003). Simulation of St. Louis, Missouri, land use impacts on thunderstorms. *Journal of Applied Meteorology*, *42*(6), 716–738. https://doi.org/10.1175/1520-0450(2003)042<0716:SOSLML>2.0.CO;2

Sen, P. K. (1968). Estimates of the regression coefficient based on Kendall's tau. *Journal of the American statistical association*, *63*(324), 1379–1389. https://doi.org/10.1080/01621459.1968.10480934

Shastri, H., Paul, S., Ghosh, S., & Karmakar, S. (2015). Impacts of urbanization on Indian summer monsoon rainfall extremes. *Journal of Geophysical Research: Atmospheres*, *120*, 496–516. https://doi.org/10.1002/2014JD022061

Sheffield, J., Goteti, G., & Wood, E. F. (2006). Development of a 50-year high-resolution global dataset of meteorological forcings for land surface modeling. *Journal of Climate*, *19*(13), 3088–3111. https://doi.org/10.1175/JCLI3790.1

Shem, W., & Shepherd, M. (2009). On the impact of urbanization on summertime thunderstorms in Atlanta: Two numerical model case studies. *Atmospheric Research*, *92*(2), 172–189. https://doi.org/10.1016/j.atmosres.2008.09.013

Tse, J. W. P., Yeung, P. S., Fung, J. C.-H., Ren, C., Wang, R., Wong, M. M.-F., & Meng, C. (2018). Investigation of the meteorological effects of urbanization in recent decades: A case study of major cities in Pearl River Delta. *Urban Climate*, *26*, 174–187. https://doi.org/10.1016/j.uclim.2018.08.007

Tumanov, S., Stan-Sion, A., Lupu, A., Soci, C., & Oprea, C. (1999). Influences of the city of Bucharest on weather and climate parameters. *Atmospheric Environment*, *33*(24-25), 4173–4183. https://doi.org/10.1016/S1352-2310(99)00160-0

Ventura, V., Paciorek, C. J., & Risbey, J. S. (2004). Controlling the proportion of falsely rejected hypotheses when conducting multiple tests with climatological data. *Journal of Climate*, *17*(22), 4343–4356. https://doi.org/10.1175/3199.1

Wai, K., Wang, X., Lin, T., Wong, M., Zeng, S., He, N., et al. (2017). Observational evidence of a long-term increase in precipitation due to urbanization effects and its implications for sustainable urban living. *Science of The Total Environment*, *599*, 647–654.

Wang, D., Jiang, P., Wang, G., & Wang, D. (2015). Urban extent enhances extreme precipitation over the Pearl River Delta, China. *Atmospheric Science Letters*, *16*(3), 310–317. https://doi.org/10.1002/asl2.559

Wang, Y., & Zhou, L. (2005). Observed trends in extreme precipitation events in China during 1961–2001 and the associated changes in large-scale circulation. *Geophysical Research Letters*, *32*, L17708. https://doi.org/10.1029/2005GL023769

Yang, K., He, J., Tang, W., Qin, J., & Cheng, C. C. (2010). On downward shortwave and longwave radiations over high altitude regions: Observation and modeling in the Tibetan Plateau. *Agricultural and Forest Meteorology*, *150*(1), 38–46. https://doi.org/10.1016/j.agrformet.2009.08.004

Yu, R., Zhou, T., Xiong, A., Zhu, Y., & Li, J. (2007). Diurnal variations of summer precipitation over contiguous China. *Geophysical Research Letters*, *34*, L01704. https://doi.org/10.1029/2006GL028129

Zhai, P., Zhang, X., Wan, H., & Pan, X. (2005). Trends in total precipitation and frequency of daily precipitation extremes over China. *Journal of climate*, *18*(7), 1096–1108. https://doi.org/10.1175/JCLI-3318.1

Zhao, Y., Zou, X., Cao, L., & Xu, X. (2014). Changes in precipitation extremes over the Pearl River Basin, southern China, during 1960–2012. *Quaternary International*, *333*, 26–39. https://doi.org/10.1016/j.quaint.2014.03.060

Zhu, Z., Zheng, B., & He, Q. (2011). Study on evolution of spatial structure of Pearl River Delta urban agglomeration and its effects. *Economic Geography*, *31*(3), 404–408.